Inorganica Chimica Acta, 204 (1993) 15–26

Indenyl hapticity in (η-indenyl–RhL$_2$) and Cr(CO)$_3$(μ-η:η-indenyl–RhL$_2$) complexes. A ^{1}H, ^{13}C and ^{103}Rh NMR spectroscopic study

Alberto Ceccon[a], Cornelis J. Elsevier[b], Jan M. Ernsting[b], Alessandro Gambaro[a], Saverio Santi[a] and Alfonso Venzo[c]
[a]*Dipartimento di Chimica Fisica, Università di Padova, via Loredan 2, 35131 Padua (Italy)*
[b]*Anorganisch Chemisch Laboratorium, Universiteit van Amsterdam, Nieuwe Achtergracht 166, 1018WV Amsterdam (Netherlands)*
[c]*CNR, Centro di Studio sugli Stati Molecolari, Radicalici ed Eccitati, via Loredan 2, 35131 Padua (Italy)*

(Received July 27, 1992)

Abstract

A series of indenyl- and (Cr(CO)$_3$)indenyl–RhL$_2$ complexes (L$_2$ = COD, (CO)$_2$) bearing substituents on both the six- and five-membered ring have been synthesized and fully characterized, and their ^{1}H, ^{13}C and ^{103}Rh NMR spectra recorded. The changes of the spectral parameters caused by the introduction of the Cr(CO)$_3$ unit suggest significant modifications of the electronic distribution in the indenyl moiety induced in the ground state. The increased reactivity in the ligand exchange reactions ('extra-indenyl effect') and the strong modifications of the catalytic and spectroscopic properties of the Rh center itself indicate a substantial weakening of the coordinative bond between rhodium and the indenyl moiety in the heterobimetallic species as expected on going from an η^5 towards a more pronounced η^3 coordination mode.

Introduction

The change of hapticity in metal–arene complexes is a topic of substantial interest in determining the reactivity and the catalytic activity of the metal core, and the associated phenomenon of ring slippage has been thoroughly studied [1].

It is well known, for example, that [(η-indenyl)]ML$_2$ complexes (M = Rh, Co; L$_2$ = COD) display enhanced catalytic activity in cyclotrimerization of alkynes to benzenes with respect to the cyclopentadienyl analogues [1–3]; in addition, it has been found that the indenyl complexes are far more reactive also in ligand substitution reactions. In the elegant study of Basolo and co-workers on the associative substitution reactions of cyclopentadienyl- and indenyl-M(CO)$_n$ complexes [3], the huge rate enhancement displayed by the indenyl derivatives ($\simeq 10^8$ times, the 'indenyl effect') was attributed to a stabilization of the transition state structure in the case of the indenyl ligand due to its greater coordinative flexibility as compared to that of the Cp one. The slippage of the metal, in fact, from an η^5 to an η^3 coordination may induce an increase of the aromatic character of the benzene ring. Conversely, the same process would produce the disruption of the aromatic character of the five-membered ring to form an allyl-ene electronic structure of higher energy in the case of the cyclopentadienyl species.

As an alternative to this interpretation, the increased reactivity in solution of indenyl versus cyclopentadienyl complexes could be due to a reduced strength of the η^5-indenyl–M bond in the *ground* state. In spite of the larger number of kinetic [4] and X-ray structural determinations [5] on indenyl–ML$_n$ complexes, until very recently there were no thermodynamic data available to evaluate the ground state M–indenyl bond strength. In a very recent paper, calorimetric measurements have shown that indenyl anionic and indenyl hydrido complexes are less stable by 10–15 Kcal/mol than the corresponding Cp analogues [6]. Thus, if that is the case, the ground state energy of these systems also contribute substantially to the 'indenyl effect'.

As a part of our studies on indenyl metal chemistry [7], we have recently reported the synthesis and X-ray structure of the heterobimetallic species Cr(CO)$_3$–(μ-η:η-indenyl)Rh(η^4-COD) (R = R' = H) [8], and later we have demonstrated that this complex, when compared with the monometallic (η-indenyl)Rh(η^4-COD), is a much more efficient catalyst in the cyclotrimerization of alkynes, and behaves quite differently in ligand substitution reactions [9]. In addition, kinetic measure-

0020-1693/93/$6.00

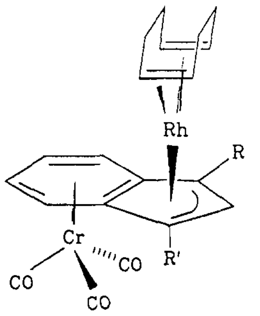

ments carried out in our laboratory have shown that the rate of substitution of CO by olefins in the bimetallic $Cr(CO)_3$–indenyl–$Rh(CO)_2$ complex is at least three orders of magnitude higher than that of the monometallic analogue [10]. This 'extra'-indenyl effect, caused by the coordination of the free benzene ring by $Cr(CO)_3$, is not accounted for by the solid state structure of the two species since the geometrical parameters of the rhodium–Cp ring moiety in the bimetallic species are very similar to those found for the monometallic one [11].

In order to obtain more insight about the indenyl hapticity in solution, we have carried out a detailed ^1H and ^{13}C spectroscopic study in solution of a series of indenyl–RhL_2 complexes bearing substituents on both the six- and five-membered ring. Compounds with L_2 = COD or L = CO as such and their $Cr(CO)_3$ complexes have been investigated. We reasoned also that hapticity changes should be cleanly reflected in $\delta(^{103}Rh)$, as small changes in the coordination sphere usually result in significant changes in the paramagnetic contribution to the chemical shift of transition metal nuclei. Hence, ^{103}Rh chemical shift data of selected compounds in the series have been acquired.

Results

Metallation of the uncomplexed indenes carried out with KH in THF at room temperature produced the quantitative formation of the corresponding indenyl anions. Reaction of these solutions with $[Rh(COD)Cl]_2$ according to published procedures [2] afforded the indenyl–Rh(COD) complexes in $\geqslant 70\%$ yields after column chromatography on silica and crystallization from pentane at low temperature.

The $Cr(CO)_3$–indenes were metallated at −30 °C in order to avoid the fast $\eta^6 \rightarrow \eta^5$ haptotropic rearrangement of the η^6-$Cr(CO)_3$ anions [7] as the η^5 isomer was found to give side products in the reaction with the Rh dimer. In particular, 1,3-Me_2–indene–$Cr(CO)_3$ was metallated in the presence of 18-crown-6 ether to ensure the quantitative transformation into the corresponding η^6 anion. The chromatographic purification of the bimetallic species was not possible because of their fast decomposition on silica, and pure compounds were obtained by repeated crystallizations from a diethyl ether–hexane mixture. The IR spectrum of all these species is characterized by two strong absorption bands in the $\nu(C{\equiv}O)$ region 2000–1800 cm^{-1} (see 'Experimental'), and in the 70 eV electron impact mass spectrum the molecular M^+ ion is detectable for all substrates.

Treatment of the parent, of the 5-NO_2-substituted and of the $Cr(CO)_3$–indenyl–Rh(COD) complexes with CO in methylene chloride solution as described in 'Experimental' gave the corresponding indenyl–$Rh(CO)_2$ derivatives in almost quantitative yield. The microcrystalline orange–brown compounds were stable in the solid state only; on the contrary, with the exception of the nitro derivative, in solution they showed appreciable decomposition, especially in coordinating solvents. The IR spectrum of these species characteristically exhibits two medium intensity bands in the 2060–1950 cm^{-1} region due to the stretching modes of the C≡O units bonded to the Rh metal together with the very strong bands typical of the $Cr(CO)_3$ unit in the 1970–1850 cm^{-1} region.

NMR measurements on the R,R'-indenyl–Rh(COD) derivatives

The ^1H and ^{13}C NMR spectra together with the mass spectroscopy data allowed the unambigous characterization of all the complexes reported. The proton assignment was performed by selective decoupling and $\{^1H\}\,^1H$ NOE measurements. The proton chemical shifts for each molecule are listed in Table 1. Among the indenyl protons, in all the investigated substrates, only H(2) is coupled measurably to ^{103}Rh nucleus ($J = c.$ 2 Hz), in agreement with a previous report [2]. The proton–proton and proton–rhodium coupling constants, as obtained by the computer simulation of the spectra, are listed in Table 2. A relatively small coupling constant (*c.* 2 Hz, on average) was measured also between the Rh atom and the olefinic hydrogen atoms of COD. The ^{13}C NMR resonances were attributed to the corresponding nuclei by using selective proton decoupling experiments and partially relaxed spectra, and the chemical shift values are reported in Table 3 together with the $^1J(^{13}C–^1H)$ and the $^1J(^{103}Rh–^{13}C)$ coupling constants.

^1H and ^{13}C data

The ^1H spectrum of the parent monometallic species exhibits an AA'BB' pattern in the range 7.3–7.1 ppm due to the benzene protons H(4)–H(7). The lower field components are slightly broadened by small coupling constants with the H(1,3) protons, so they are attributed

TABLE 1. ^{1}H NMR chemical shifts[a,b] for indenyl potassium and R,R'-indenyl–RhL$_2$ complexes

Compound				Indenyl protons							COD protons	
No.	L$_2$	R	R'	H(1)	H(2)	H(3)	H(4)	H(5)	H(6)	H(7)	=C–H	CH$_2$
1	COD	Me	Me		5.800		7.155	7.080	7.080	7.155	3.36	1.87 and 1.73
2	COD	Me	H		5.925	5.033	7.177	7.050	7.088	7.195	3.51 and 3.81	≃1.8 and ≃1.7
3	COD	H	H	5.161	6.091	5.161	7.230	7.064	7.064	7.230	3.96	1.83 and 1.71
4	COD	Ph	H		6.375	5.124	7.307	7.127	7.154	7.585	3.42 and 3.87	1.88 and 1.71
5	COD	Ph	Ph		6.722		7.699	7.218	7.218	7.699	3.29	≃1.9 and ≃1.7
6	COD	H	H	5.304	6.378	5.375	8.225		7.883	7.194	4.26 and 4.07	≃1.9 and ≃1.7
7	COD	Me	Me		6.035		5.955	5.234	5.234	5.955	3.70	≃2.0 and ≃1.8
8	COD	Me	H		6.202	4.939	6.000	5.219	5.240	5.959	4.11 and 3.82	≃2.0 and ≃1.8
9	COD	H	H	5.066	6.403	5.066	6.014	5.227	5.227	6.014	4.25	≃2.0 and ≃1.8
10	COD	Ph	H		6.637	5.043	6.107	5.253	5.318	6.285	4.16 and 3.71	≃2.0 and ≃1.8
11	COD	Ph	Ph		6.909		6.406	5.352	5.352	6.406	3.58	≃2.0 and ≃1.8
12	(CO)$_2$	H	H	5.840	6.107	5.840	7.295	7.137	7.137	7.295		
13	(CO)$_2$	H	H	5.959	6.393	5.967	8.198		7.957	7.359		
14	(CO)$_2$	H	H	5.745	6.439	5.745	5.920	5.177	5.177	5.920		
15	Indenyl$^-$K$^+$ [c]			5.735	6.362	5.735	7.169	6.319	6.319	7.169		

[a] Solvent, CD$_2$Cl$_2$, δ (ppm) from internal Me$_4$Si, $T = 298$ K. The uncertainties in chemical shift values are $\leqslant 0.001$ ppm. [b] Others: compound **1**, δ(CH$_3$) 1.873; compound **2**, δ(CH$_3$) 1.900; compound **4**, $\delta(o,o')$ 7.531, $\delta(m,m')$ 7.388, $\delta(p)$ 7.249; compound **5**, $\delta(o,o')$ 7.602, $\delta(m,m')$ 7.411, $\delta(p)$ 7.270; compound 7, δ(CH$_3$) 1.843; compound **8**, δ(CH$_3$) 1.973; compound **10**, $\delta(o,o')$ 7.510, $\delta(m,m')$ 7.445, $\delta(p)$ 7.328; compound **11**, $\delta(o,o')$ 7.572, $\delta(m,m')$ 7.474, $\delta(p)$ 7.354. [c] Solvent, THF-d$_8$, $T = 240$ K.

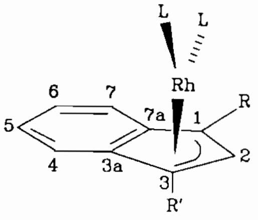

1–5, 12

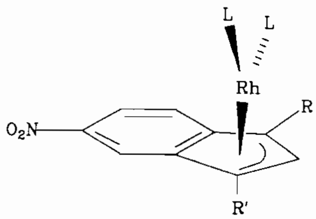

6, 13

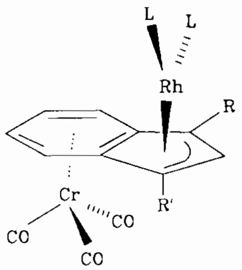

7–11, 14

to H(4) and H(7), and these assignments were confirmed by NOE experiments. The lower field positions of the signals due to the H(4,7) nuclei with respect to the H(5,6) nuclei is a common feature of all the Rh(I)L$_2$ complexes studied in this work. Besides these signals, an AA'X spin system is present in the range 6.1–5.1 ppm due to the H(2) and H(1,3) protons, the former showing a 2.00 Hz coupling constant with the Rh nucleus. The resonance arising from the COD olefinic protons appears as a broad singlet at 3.96 ppm, and the methylene signals are detected between 1.9 and 1.7 ppm. The ^{13}C NMR spectrum is consistent with the molecular structure of this complex. It is remarkable that the ^{103}Rh nucleus couples with all the carbon atoms of the five-membered ring as well as with the COD olefinic ones.

Upon substitution of H(1) with a methyl or a phenyl group the molecular symmetry of the complexes is lowered and an ABCD spin system is observed for the benzo protons and an AX one for the Rh-coordinated five-membered ring protons, where the X component (i.e., the H(2) proton) shows the coupling with Rh. A small upfield shift is generally measured for the indenyl proton resonances due to the -I effect of the methyl group, whereas the opposite effect found for the H(4,7) and H(2) proton chemical shift induced by phenyl substituents in the 1,3-positions may be due mainly to the presence of anisotropic ring currents in the phenyl ring(s), and the downfield direction of the shifts reveals a preferred co-planar conformation of the phenyl and indenyl frameworks [7]. Two well distinct signals also appear for the COD olefinic hydrogen atoms owing to the prochiral nature of the unsymmetrically substituted indenyl unit. Substitution of both the H(1,3) hydrogen atoms with methyl or phenyl groups restores the molecular symmetry of the parent compound and increases the electronic effect of the substituents. The chemical shift variations observed upon introduction of an NO$_2$ group in the 5-position are consistent with the strong electron withdrawing effect of such a substituent.

Substitution of two C≡O groups for COD both in indenyl- and 5-NO$_2$-indenyl rhodium derivatives induced a downfield shift in the cyclopentadienyl moiety proton resonances (in particular, H(1) and H(3)) with

TABLE 2. $J(i,j)$ proton–proton and proton–rhodium coupling constants (uncertainties in parentheses)[a] for the indenyl potassium and the R,R′-indenyl–RhL$_2$ complexes **1–15**

i,j	Compound no.														
	1[b]	**2**[c]	**3**	**4**[d]	**5**[e]	**6**	**7**[f]	**8**[g]	**9**	**10**[h]	**11**[i]	**12**	**13**	**14**	**15**
1,2			2.82(0.01)			2.89(0.01)			2.93(0.01)			2.99(0.01)	3.04(0.01)	3.11(0.01)	3.37(0.01)
1,3			2.87(0.02)			1.51(0.01)			2.85(0.02)			2.98(0.02)	1.77(0.01)	3.12(0.01)	2.55(0.04)
1,4			1.20(0.01)			0.76(0.01)			0.99(0.01)			0.79(0.01)	0.80(0.01)	0.98(0.01)	1.16(0.02)
1,7			−0.62(0.01)			0.00(0.01)			−0.56(0.01)			0.00(0.02)	0.00(0.01)	−0.22(0.01)	−0.61(0.02)
2,3		2.71(0.01)	2.82(0.01)	2.90(0.02)		2.88(0.01)		2.88(0.01)	2.93(0.01)	3.01(0.01)		2.99(0.01)	3.04(0.01)	3.11(0.01)	3.37(0.01)
2,Rh	2.10(0.01)	2.14(0.01)	2.00(0.01)	1.83(0.02)	1.87(0.02)	2.02(0.01)	1.90(0.03)	2.13(0.01)	2.10(0.01)	2.08(0.02)	2.13(0.02)	2.40(0.02)	2.42(0.01)	2.71(0.01)	
3,4		0.00(0.01)	−0.62(0.01)	0.00(0.02)		0.00(0.01)		0.00(0.01)	−0.56(0.01)	0.00(0.01)		0.00(0.02)	0.00(0.01)	−0.22(0.01)	−0.61(0.02)
3,7		0.80(0.02)	1.20(0.01)	0.77(0.02)		0.75(0.01)		0.81(0.01)	0.99(0.01)	0.75(0.01)		0.79(0.01)	0.79(0.01)	0.98(0.01)	1.16(0.02)
4,5	8.23(0.05)	8.15(0.02)	8.24(0.01)	8.07(0.02)	8.38(0.02)		6.91(0.08)	6.78(0.01)	6.78(0.01)	6.77(0.01)	6.95(0.03)	8.05(0.01)		6.62(0.01)	8.01(0.01)
4,6	1.06(0.05)	1.06(0.02)	1.00(0.01)	1.11(0.02)	1.05(0.03)	2.13(0.01)	0.83(0.08)	1.00(0.01)	0.93(0.01)	0.96(0.01)	0.87(0.03)	1.01(0.01)	2.10(0.01)	0.96(0.01)	1.15(0.01)
4,7	0.93(0.05)	0.80(0.02)	0.96(0.01)	0.80(0.02)	0.92(0.02)	0.73(0.01)	0.59(0.09)	0.65(0.01)	0.56(0.01)	0.62(0.01)	0.49(0.03)	0.93(0.02)	0.72(0.01)	0.59(0.01)	0.83(0.02)
5,6	6.86(0.05)	6.86(0.01)	6.84(0.01)	6.87(0.02)	6.87(0.03)		5.99(0.09)	6.09(0.01)	6.04(0.01)	6.02(0.01)	5.97(0.03)	7.09(0.02)		6.21(0.01)	6.49(0.02)
5,7	1.06(0.05)	1.06(0.02)	1.00(0.01)	1.14(0.02)	1.05(0.03)		0.83(0.08)	1.04(0.01)	0.93(0.01)	0.89(0.01)	0.87(0.03)	1.01(0.01)		0.96(0.01)	1.15(0.01)
6,7	8.23(0.05)	8.22(0.02)	8.24(0.01)	8.23(0.03)	8.38(0.02)	8.96(0.01)	6.91(0.08)	6.76(0.01)	6.78(0.01)	6.94(0.01)	6.95(0.03)	8.05(0.01)	8.86(0.01)	6.62(0.01)	8.01(0.01)

[a] Values in Hz. For proton labelling, see Table 1. [b] Compound **1**, $J(2,\mathrm{CH}_3)$ 0.55(0.01) Hz. [c] Compound **2**, $J(2,\mathrm{CH}_3)$ 0.59(0.01) Hz. [d] Compound **4**, phenyl protons: $J(o,m)=J(o',m')$ 7.81(0.06); $J(o,p)=J(o',p)$ 1.21(0.05); $J(o,m')=J(o',m)$ 0.53(0.06); $J(o,o')$ 2.07(0.08); $J(m,p)=J(m',p)$ 7.42(0.05); $J(m,m')$ 1.43(0.09) Hz. [e] Compound **5**, phenyl protons: $J(o,m)=J(o',m')$ 7.85(0.01); $J(o,p)=J(o',p)$ 1.23(0.01); $J(o,m')=J(o',m)$ 0.57(0.01); $J(o,o')$ 2.00(0.02); $J(m,p)=J(m',p)$ 7.43(0.01); $J(m,m')$ 1.46(0.02) Hz. [f] Compound **7**, $J(2,\mathrm{CH}_3)$ 0.60(0.08) Hz. [g] Compound **8**, $J(2,\mathrm{CH}_3)$ 0.68(0.01) Hz. [h] Compound **10**, phenyl protons: $J(o,m)=J(o',m')$ 7.86(0.03); $J(o,p)=J(o',p)$ 1.25(0.02); $J(o,m')=J(o',m)$ 0.58(0.03); $J(o,o')$1.97(0.04; $J(m,p)=J(m',p)$ 7.47(0.02); $J(m,m')$ 1.47(0.04) Hz. [i] Compound **11**, phenyl protons: $J(o,m)=J(o',m')$ 7.84(0.05); $J(o,p)=J(o',p)$ 1.15(0.04); $J(o,m')=J(o',m)$ 0.52(0.05); $J(o,o')$ 2.00(0.07); $J(m,p)=J(m',p)$ 7.49(0.04); $J(m,m')$ 1.51(0.07) Hz.

TABLE 3. ^{13}C NMR parameters[a,b] for the free, η^6- and η^5-indenyl potassium salts[c], and for the R,R′-indenyl–RhL$_2$ complexes[d]

Compound				Indenyl carbons									COD carbons	
No.	L$_2$	R	R′	C(1)	C(2)	C(3)	C(3a)	C(4)	C(5)	C(6)	C(7)	C(7a)	=C–H	CH$_2$
1	COD	Me	Me	85.82	95.59	85.82	112.80	117.87	122.19	122.19	117.87	112.80	71.27	31.73
				(–)	(170)	(–)	(–)	(162)	(159)	(159)	(162)	(–)	(151)	(127)
				[4.9]	[5.5]	[4.9]	[2.5]	[–]	[–]	[–]	[–]	[2.5]	[14.0]	[–]
2	COD	Me	H	88.43	93.93	73.86	113.16	119.66	122.52	122.28	117.84	113.42	70.92; 68.03	32.13; 31.27
				(–)	(172)	(173)	(–)	(159)	(159)	(159)	(159)	(–)	(155; 140)	(125; 130)
				[4.3]	[5.2]	[4.6]	[2.7]	[–]	[–]	[–]	[–]	[2.2]	[13.4; 14.0]	[–]
3	COD	H	H	76.52	92.90	76.52	113.61	119.76	122.71	122.71	119.76	113.61	67.86	31.70
				(173)	(175)	(173)	(–)	(173)	(170)	(170)	(173)	(–)	(155)	(127)
				[4.6]	[4.9]	[4.6]	[2.4]	[–]	[–]	[–]	[–]	[2.4]	[13.4]	[–]
4	COD	Ph	H	94.57	92.75	75.19	114.07	120.54	123.30	122.75	118.42	111.56	72.98; 68.95	31.53; 31.79
				(–)	(173)	(175)	(–)	(162)	(158)	(163)	(159)	(–)	(156; 152)	(128; 126)
				[4.0]	[5.0]	[4.7]	[2.4]	[–]	[–]	[–]	[–]	[2.0]	[13.4; 14.0]	[–]
5	COD	Ph	Ph	92.83	92.75	92.83	111.86	119.27	123.37	123.37	119.27	111.86	73.82	31.57
				(–)	(172)	(–)	(–)	(158)	(159)	(159)	(158)	(–)	(155)	(129)
				[4.3]	[4.9]	[4.3]	[1.8]	[–]	[–]	[–]	[–]	[1.8]	[14.0]	[–]
6	COD	H	H	77.82	97.99	78.35	115.26	116.86	142.73	117.69	118.82	111.59	70.75; 69.81	31.64; 31.35
				(175)	(176)	(176)	(–)	(167)	(–)	(167)	(164)	(–)	(154; 151)	(128; 126)
				[3.8]	[5.4]	[3.8]	[2.3]	[–]	[–]	[–]	[–]	[2.3]	[13.0; 13.0]	[–]
7	COD	Me	Me	85.48	105.63	85.48	85.82	84.83	90.28	90.28	84.83	85.83	74.16	31.48
				(–)	(173)	(–)	(–)	(174)	(173)	(173)	(174)	(–)	(156)	(127)
				[4.5]	[6.0]	[4.5]	[2.7]	[–]	[–]	[–]	[–]	[2.7]	[13..5]	[–]
8	COD	Me	H	88.04	104.56	72.56	87.33	84.85	90.21	90.54	86.34	86.16	74.04; 71.25	31.80; 31.09
				(–)	(175)	(171)	(–)	(171)	(172)	(172)	(173)	(–)	(151; 154)	(127; 128)
				[3.1]	[5.2]	[4.3]	[1.8]	[–]	[–]	[–]	[–]	[1.5]	[13.4; 13.4]	[–]
9	COD	H	H	75.19	104.19	75.19	87.52	85.97	90.49	90.49	85.97	87.52	71.35	31.70
				(180)	(177)	(180)	(–)	(176)	(173)	(173)	(176)	(–)	(155)	(129)
				[4.5]	[5.4]	[4.5]	[2.2]	[–]	[–]	[–]	[–]	[2.2]	[13.5]	[–]
10	COD	Ph	H	93.80	103.26	73.52	86.86	84.51	90.95	90.07	86.67	88.62	76.10; 72.24	31.43; 31.34
				(–)	(176)	(177)	(–)	(175)	(173)	(173)	(174)	(–)	(153; 154)	(127; 127)
				[3.1]	[5.3]	[4.3]	[4.0]	[–]	[–]	[–]	[–]	[3.1]	[13.3; 13.3]	[–]
11	COD	Ph	Ph	91.80	102.49	91.80	85.35	85.16	90.60	90.60	85.16	85.35	76.93	31.35
				(–)	(175)	(–)	(–)	(174)	(173)	(173)	(174)	(–)	(156)	(128)
				[3.1]	[6.5]	[3.1]	[2.2]	[–]	[–]	[–]	[–]	[2.2]	[13.4]	[–]
12	(CO)$_2$	H	H	76.00	98.15	76.00	117.99	119.40	125.31	125.31	119.40	117.99	–	–
				(171)	(178)	(171)	(–)	(164)	(161)	(161)	(164)	(–)	(–)	(–)
				[3.6]	[6.3]	[3.6]	[1.9]	[–]	[–]	[–]	[–]	[1.9]	[–]	[–]
13	(CO)$_2$	H	H	76.84	103.10	76.41	120.41	115.47	145.03	120.10	119.10	116.62	–	–
				(179)	(180)	(179)	(–)	(170)	(–)	(168)	(167)	(–)	(–)	(–)
				[3.6]	[6.1]	[3.6]	[2.0]	[–]	[–]	[–]	[–]	[2.0]	[–]	[–]
14	(CO)$_2$	H	H	74.87	110.22	74.87	91.03	85.02	91.12	91.12	85.02	91.03	–	–
				(182)	(181)	(182)	(–)	(174)	(174)	(174)	(174)	(–)	(–)	(–)
				[3.1]	[6.1]	[3.1]	[1.3]	[–]	[–]	[–]	[–]	[1.3]	[–]	[–]
15	Indenyl$^-$K$^+$			93.51	117.75	93.51	129.16	119.00	113.32	113.32	119.00	129.16	–	–
				(160)	(155)	(160)	(–)	(149)	(155)	(155)	(149)	(–)	(–)	(–)
				[–]	[–]	[–]	[–]	[–]	[–]	[–]	[–]	[–]	[–]	[–]
16	η^6-Cr(CO)$_3$–indenyl$^-$K$^+$			95.70	128.25	95.70	108.76	92.94	84.50	84.50	92.94	108.76	–	–
				(162)	(153)	(162)	(–)	(162)	(169)	(169)	(162)	(–)	(–)	(–)
				[–]	[–]	[–]	[–]	[–]	[–]	[–]	[–]	[–]	[–]	[–]
17	η^5-Cr(CO)$_3$–indenyl$^-$K$^+$			72.55	90.06	72.55	107.25	125.86	120.33	120.33	125.86	107.25	–	–
				(174)	(170)	(174)	(–)	(160)	(157)	(157)	(160)	(–)	(–)	(–)
				[–]	[–]	[–]	[–]	[–]	[–]	[–]	[–]	[–]	[–]	[–]

[a] δ (ppm) from internal Me$_4$Si, $T = 298$ K unless otherwise indicated, ^1J(C–H) (in parentheses) and ^1J(^{103}Rh–C) (in brackets) (Hz). The uncertainties in chemical shift and coupling constant values are $\leqslant 0.01$ ppm and $\leqslant 0.3$ Hz, respectively. For carbon labelling, see Table 1.

[b] Others: compound **1**, δ(CH$_3$) 10.38 (J 127 Hz); compound **2**, δ(CH$_3$) 10.54 (126); compound **4**, $\delta(o,o')$ 127.67 (158); phenyl carbons: $\delta(m,m')$ 129.01 (161); $\delta(p)$ 126.97 (161); $\delta(j)$ 136.38; compound **5**, phenyl carbons: $\delta(o,o')$ 127.75 (160); $\delta(m,m')$ 129.09 (162); $\delta(p)$ 126.08 (162); $\delta(j)$ 135.96; compound **7**, δ(Cr($C{\equiv}O$)$_3$) 235.01; δ(CH$_3$) 10.12 (J 129 Hz); compound **8**, δ(CH$_3$) 10.28 (J 128 Hz); δ(Cr($C{\equiv}$O)$_3$) 234.95; compound **9**, δ(Cr($C{\equiv}$O)$_3$) 234.87; compound **10**, δ(Cr($C{\equiv}$O)$_3$) 234.58; phenyl carbons: $\delta(o,o')$ 127.67 (158); $\delta(m,m')$ 129.34 (161); $\delta(p)$ 127.54 (158); $\delta(j)$ 133.96; compound **11**, δ(Cr($C{\equiv}$O)$_3$) 234.19; phenyl carbons: $\delta(o,o')$ 127.70 (163); $\delta(m,m')$ 129.44(161); $\delta(p)$ 127.54 (160); $\delta(j)$ 133.58; compound **12**, δ(Rh($C{\equiv}$O)$_2$) 190.49 [86.2]; compound **13**, δ(Rh($C{\equiv}$O)$_2$) 188.45 [86.0]; compound **14**, δ(Cr($C{\equiv}$O)$_3$) 233.55; δ(Rh($C{\equiv}$O)$_2$) 187.90 [86.2]; compound **16**, δ(Cr($C{\equiv}$O)$_3$) 241.65; compound **17**, δ(Cr($C{\equiv}$O)$_3$) 246.05.

[c] Solvent, THF-d$_8$. For the η^6-Cr(CO)$_3$–indenyl potassium salt, $T = 240$ K.

[d] Solvent, CD$_2$Cl$_2$, $T = 298$ K.

minor effects on the chemical shift values of the protons in the other positions. At the same time, a noticeable downfield shift is also experienced by the ^{13}C resonances attributed to the C(2), C(3a) and C(7a) carbon atoms, the chemical shifts of the other carbon nuclei being very slightly affected. The ^{13}C NMR spectra of the monometallic indenyl–RhL_2 species are consistent with the proposed molecular structure of these compounds.

Coordination of the benzo ring with $Cr(CO)_3$ induces the well-known upfield shift (*c.* 1.2–2 ppm) of the corresponding proton resonances. Minor effects are observed for the H(1–3) chemical shift, even if the variation generally found is a downfield shift for H(2) and a upfield shift for H(1,3) so that the differences $\Delta\delta(^1H) = \delta_{H(2)} - \delta_{H(3)}$ markedly increase. Moreover, the presence of $Cr(CO)_3$ induces a significant downfield shift of the resonance belonging to the COD olefinic protons.

The ^{13}C NMR chemical shifts are also modified by $Cr(CO)_3$ in the usual way, i.e. the resonances of the protonated carbon atoms of the Cr-complexed benzo ring are shifted upfield by 32 ppm and those of the quaternary ones by 28 ppm (on average). As found for the ^1H chemical shifts, the complexation with $Cr(CO)_3$ induces a substantial increase in the differences of chemical shift values $\Delta\delta(^{13}C) = \delta_{C(2)} - \delta_{C(3)}$.

^{103}Rh NMR data

As has been previously reported [12], the inverse 2D detection technique is the one of choice for quick access to ^{103}Rh NMR spectra. In our compounds the measurements could be carried out successfully by using the inverse ^1H, ^{103}Rh 2D experiments because of the presence of a coupling constant of *c.* 2 Hz between the H atom at the indenyl 2-position and ^{103}Rh. The acquired data have been collected in Table 4, together with known data of several related compounds. A typical 2D spectrum is shown in Fig. 1, where the vertical trace (F1) shows the ^{103}Rh NMR spectrum and the horizontal trace (F2) gives the ^1H NMR spectrum of protons coupled to Rh by approximately the input *J* value, i.e. only H(2).

TABLE 4. ^{103}Rh NMR chemical shifts[a] for the R,R′-indenyl–RhL_2 (L_2 = COD, $(CO)_2$) complexes, together with known data of some related compounds

Compound			$\delta(^{103}Rh)$[b]	
No.	R	R′	L_2 = COD	$L_2 = (CO)_2$
1	Me	Me	−529	
2	Me	H	−510	
3	H	H	−487	−1038
4	Ph	H	−437	
5	Ph	Ph	−392	
6	H	H	−413	−987
7	Me	Me	−420	
9	H	H	−358	−931
11	Ph	Ph	−278	
(η-cyclopentadienyl)RhL_2			−777[c]	−1321[d]
(η-cyclooctenyl)RhL_2			−9[c]	

[a] For the experimental details of data acquisition, see 'Experimental'. For the complex identification, see Table 1. [b] ppm, ±1. [c] Data from ref. 15. [d] Data from ref. 18.

Discussion

^{103}Rh NMR

The ^{103}Rh chemical shift values of rhodium complexes cover a very wide range from *c.* +10000 ppm for the Rh(III) complexes to *c.* −2200 ppm for the more shielded formal Rh(0) ones [13, 14]. The δ(Rh) of the presented Rh(I) complexes is expected to depend heavily upon the nature of the aromatic or allylic systems coordinated to the metal as well as upon the ancillary ligands (phosphines, olefins, CO, etc.). For example, the ^{103}Rh nucleus resonates at δ −487 ppm in the (η-indenyl)Rh(COD) complex (see Table 3) and at *c.* −650 ppm in the (η-indenyl)$Rh(C_2H_4)_2$ analogue [15]. Similarly, a *c.* 220 ppm upfield shift was measured on going from the (η-cyclopentadienyl)–Rh(COD) complex (δ −777 ppm) to the (η-cyclopentadienyl)–$Rh(C_2H_4)_2$ one (δ *c.* −1000 ppm). Hence, for a correct comparison, homologous series of complexes have to be taken into account.

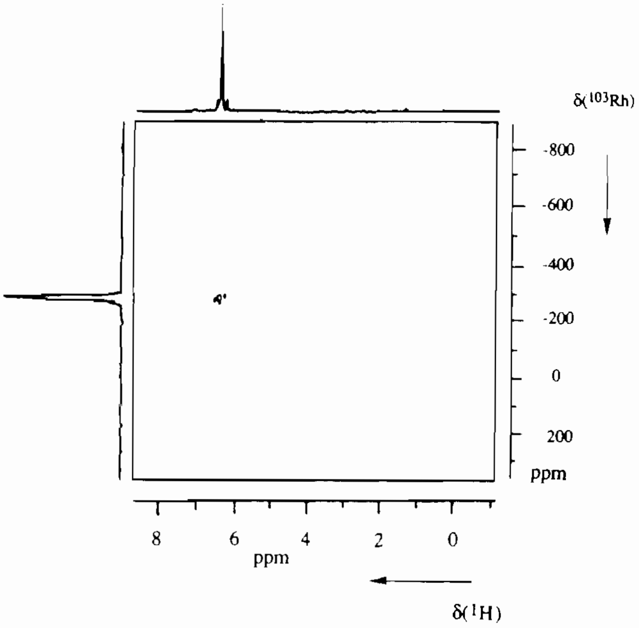

Fig. 1. Inverse 2D ^1H, ^{103}Rh NMR spectrum of (1,3-diphenyl–indenyl)Rh(COD). For the experimental conditions, see text.

The ligand hapticity and the electron density at the metal markedly affect the ^{103}Rh chemical shift values. For instance, for the η-cyclopentadienyl complex of the Rh(COD) series, which is claimed to display a quasi-perfect η^5 hapticity [16], the ^{103}Rh resonance is observed at -777 ppm, i.e. 768 ppm upfield with respect to the η-cyclooctenyl analogue [15], for which an η^3 hapticity is the only one accessible. The upfield position of the Rh resonance observed for the cyclopentadienyl derivatives may be interpreted [15] as an indication for a 18-electron rhodium species to which the Cp group is η^5-coordinated. Conversely, the downfield shift measured on going to the cyclooctenyl derivative may be due to the presence of a less shielded 16-electron Rh species [17].

In the (η-indenyl)Rh(COD) complex, the ^{103}Rh resonates at -487 ppm, i.e. an intermediate value between those of the cyclopentadienyl and cyclooctenyl derivatives. The downfield shift ($\Delta\delta$ 290 ppm) observed on replacing Cp with indenyl is of the order of that observed on going from (η-Cp)Rh(C_2H_4)$_2$ (δ *c.* -1000 ppm) to (η-indenyl)Rh(C_2H_4)$_2$ [15] (δ *c.* -650 ppm) and it may be accounted for by participation of a 16-electron rhodium species [17]. Thus, we feel that the situation may be described neither as an η^3 nor as an η^5 coordination of the indenyl group to the Rh centre, but instead by a time averaged ($\eta^3+\eta^2$) coordination. This situation should lead to a 18-electron type Rh species, too; however, the organic fragment is no longer a fully delocalized carbocycle suggesting less stabilization of the relevant π-molecular orbitals and hence a lower ΔE (on average) between the HOMO and LUMO orbitals for this type of compound compared to the corresponding (η^5-Cp)Rh complexes. The lower ΔE value will induce a relevant downfield shift of the ^{103}Rh resonances, in good accordance with the experimental data. An allylene ($\eta^3+\eta^2$) coordination of Rh has been suggested even for the η-(cyclopentadienyl)Rh(COD) complex in the solid state [16], a type of bonding less favourable in a Cp than in an indenyl ligand.

The substituent effect on δ(^{103}Rh) in the indenyl series is reported in Table 4. The observed trend is similar to that found for a series of Cp analogues published recently by Rausch and co-workers [18]. The electron-withdrawing substituents (phenyl and nitro groups) shift the resonance downfield, while the electron-releasing ones (methyl) induce an upfield shift. Of particular interest is the effect of coordination of the benzene ring with Cr(CO)$_3$; the observed downfield shift ($\Delta\delta = 129$ ppm) is markedly higher than that induced by the nitro group (74 ppm). Comparable Cr(CO)$_3$ effects on δ(^{103}Rh) have been found also for the 1,3-Me$_2$– and 1,3-Ph$_2$–indenyl-Rh(COD) complexes. Similarly, when the COD ligand was substituted by two COs, the downfield shift induced by Cr(CO)$_3$ (107 ppm) is significantly higher than that by the nitro group (51 ppm). As the electron-withdrawing effect of the Cr(CO)$_3$ and NO_2 groups as measured by a kinetic [19] or a thermodynamic [20] approach is almost equal, we conclude that Cr(CO)$_3$ induces a downfield shift of the Rh resonance which cannot be justified by its electron-withdrawing properties alone. In our opinion, therefore, the rhodium–indenyl bonding mode is different in the mono- and bis-complexed species, and this fact can be represented by an increased importance of an η^3 hapticity in the bimetallic complexes.

^{1}H and ^{13}C NMR data

It is appropriate to recall here that recently some geometric parameters, obtained by X-ray analysis, have been proposed to describe the Rh–indenyl bonding mode, and hence the hapticity, in the solid state. In this respect, several authors [5a] refer to the hinge angle, HA, between the C(1), C(2) and C(3), and the C(3a), C(3), C(4), C(5), C(6), C(7) and C(7a) least-squares planes, to the dihedral fold angle, FA, between the C(1), C(2) and C(3), and the C(1), C(3), C(3a) and C(7a) least-squares planes, and, most of all, to the slip parameter, $\Delta(\mathrm{M-C})$ (Å) $=\{[d(\mathrm{Rh{-}C_{3a}})+d(\mathrm{Rh{-}C_{7a}})]/2\text{-}[d(\mathrm{Rh{-}C_3})+d(\mathrm{Rh{-}C_1})]/2\}$ as a measure of the indenyl frame geometry variations and of the slippage of the rhodium atom away from the quarternary carbon atoms. For example, in the (indenyl)$_2$M series (M = Fe, Co, Ni) a successive increase was measured in the degree of slip-fold distortion which involves both slippage of the metal away from the quaternary carbons and folding of the five-membered ring (as expected in the presence of relevant contributions coming from an η^3 bonding mode) in the order Fe < Co < Ni [5a]. These differences in the geometrical parameters are very likely due to important modifications of the bonding mode of *different* metals with the Cp ring. On the contrary, the crystallographic parameters display almost identical values when the *same* metal is coordinated to the indenyl frame and substituents are introduced in the five- or six-membered ring, as in the case of the hepta-methyl [21] and the Cr(CO)$_3$ derivatives [8]. In contrast to the invariability of the HA, FA and $\Delta(\mathrm{M-C})$ values, it is worthwhile recalling that in solution the introduction of Cr(CO)$_3$ in this system causes a huge enhancement of the L ligand exchange rate and of the catalytic activity [9]. Therefore, it is evident that the crystallographic parameters, obtained in the solid state, are not sensitive enough to the same structural modifications as the kinetic and ^{103}Rh spectroscopic parameters obtained in solution.

Further insight into this question may be obtained from the inspection of selected NMR parameters obtained in solution. In particular, in a large series of indenyl complexes a correlation between the chemical shift values of the junction carbon atoms C(3a) and C(7a) and the hapticity has been proposed [5a, 22–24]. The upfield shift measured for these nuclei with respect to suitable references has been taken as an indication of η^5-coordination, while the downfield shift was considered diagnostic for significant distortions towards η^3-coordination. Additionally, the rather extreme low field position of the junction carbon resonances found for the [(η-indenyl)Ir(PMe$_2$Ph)$_3$) [25] (and [η-indenyl)-Fe(CO)$_3$]$^-$) [26] complexes is evidence of an η^3 hapticity, as confirmed by the X-ray measurements. In the case of the bimetallic Cr–Rh complexes, the chemical shift values of C(3a) and C(7a) carbon atoms can hardly be used to establish the Rh hapticity, since the δ values of the quaternary carbon nuclei are shifted strongly upfield (*c.* 28 ppm) by coordination with Cr(CO)$_3$ [27]. Thus, in order to obtain more information on the electronic distribution, and hence on the hapticity, in these bimetallic species we took into consideration other spectroscopic parameters, *in casu*, Δ^3J(H,H), $\Delta\delta(^1H)$ and $\Delta\delta(^{13}C)$ (see below).

In our studies on the Cr(CO)$_3$ complexes of biphenylene [28] and of a series of arylmethyl carbanions [30–32], for example, the Δ^3J(H,H) parameter has been used in order to get information about the localization of π-electrons in the aromatic ligand. In particular, the extent of the double bond fixation has been assessed by the large value of the difference between the vicinal proton–proton coupling constants $\Delta^3J(H,H) = {}^3J_{o,m} - {}^3J_{m,p}$, and it was confirmed by X-ray analysis in the case of biphenylene [29].

In the case of the indenyl anion, the same parameter may be used to evaluate the relative weight of the two limiting structures **A** and **B**.

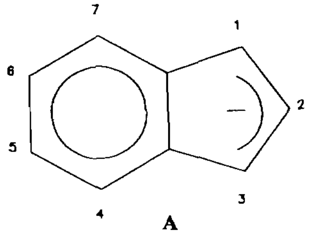

A

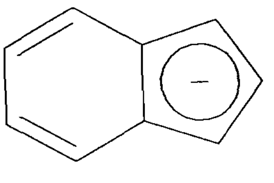

B

In fact, in a recent paper [7] we correlated the Δ^3J(H,H) difference between the $^3J_{4,5}$ and $^3J_{5,6}$ coupling constant values of the indenyl anion with the extent of double bond fixation induced by the coordination with a Cr(CO)$_3$ unit to the six- or five-membered ring. Thus, the relatively small Δ^3J(H,H) value (1.27 Hz, Table 5, no. **16**) measured when Cr(CO)$_3$ is bonded to the six-membered ring is an evidence of a low double bond fixation in the complexed ring (and hence a noticeable aromatic character) as in structure **A**. In contrast, the higher Δ^3J(H,H) values found for the free indenyl ligand (1.52 Hz) and for the η^5 species (2.09 Hz) indicate a substantial double bond fixation in the six-membered ring, for these two anions, as depicted in structure **B**. The same conclusions arise also if we consider the chemical shift values of the five-membered ring nuclei. The entities of the parameters $\Delta\delta(^1H) = \delta_{H(2)} - \delta_{H(1)}$ and $\Delta\delta(^{13}C) = \delta_{C(2)} - \delta_{C(1)}$ obtained for the free and Cr(CO)$_3$-complexed indenyl anions (see Table 5, **15**–**17**) are noticeably higher in the η^6 anion than in the free one. The greater value is mainly due to the downfield shift of the H(2) and C(2) resonances rather than to variations of the chemical shifts of H(1,3) and C(1,3) which change slightly upon complexation of the benzene ring (see Tables 1 and 3). This is just what we expect for a more pronounced allyl character of the π-electron density at C(1)–C(3), as represented in structure **A**. The haptotropic migration of the Cr(CO)$_3$ from the six- to the five-membered ring induces the well known upfield shift for both the proton and carbon resonances of the Cp fragment; however, the extent of the phenomenon is more pronounced for the H(2) and C(2) nuclei with respect to the H(1,3) and C(1,3) ones, so both $\Delta\delta(^1H)$ and $\Delta\delta(^{13}C)$ values become substantially smaller. Thus, for the free and the η^5 anion, a similar electronic distribution as that depicted in formula **B** is proposed, in good accordance with the trend of the Δ^3J(H,H) values. Another test for the validity of the $\Delta\delta$ parameter is given by the ^{13}C data obtained for the (indenyl)$_2$M series where the highest value of $\Delta\delta(^{13}C)$ was found for the Ni complex [5b], which shows a substantial departure from an η^5 towards an η^3 hapticity, as demonstrated by the X-ray data [5a].

Going back to the case of indenyl–Rh(COD) complexes, the Δ^3J(H,H) values reported in Table 5 are noticeably lower and the $\Delta\delta(^1H)$ higher when the Cr(CO)$_3$ group is bonded to the benzene ring. Meanwhile, in the bimetallic species the $\Delta\delta(^{13}C)$ values are 10–13 ppm higher and closely resemble the values recently reported for a 'true'-η^3 bis(allyl)rhodium chloride dimer in solution and in the solid state (32.0 ppm in both cases) [33]. Again the most relevant contribution to this trend comes from the strong downfield shift measured for the resonances of H(2) and C(2). As in the case of ^{103}Rh chemical shift values (see above), this effect cannot be ascribed to the electron-withdrawing effect of the Cr(CO)$_3$ group [19, 20], since the presence of a nitro group in the benzene ring increases only slightly both the $\Delta\delta(^1H)$ and the $\Delta\delta(^{13}C)$ values (see Table 5). It is well established that the magnitude of the coordination effect of Cr(CO)$_3$ on the chemical shifts of the nuclei belonging to a side chain (and, in particular, to the β positions) is very small [34]. Thus, the effect of the coordination of Cr(CO)$_3$ on the H(2) and C(2) chemical shifts may arise from the influence of chromium on the extended π-electron distribution. The quenching effects of

TABLE 5. Selected ^1H and ^{13}C NMR parameters[a] for the free, η^6 and η^5-$Cr(CO)_3$–indenyl anions, and for the R,R'-indenyl–RhL_2 (L_2 = COD, $(CO)_2$) complexes

Compound				$\Delta^3J(H,H)$ (Hz)	$\Delta\delta(^1H)$ (ppm)	$\Delta\delta(^{13}C)$ (ppm)	Reference
No.	R	R'	L_2				
1	Me	Me	COD	1.37		9.77^b	^{e}
3	H	H	COD	1.40	0.93	16.38	8, ^{e}
5	Ph	Ph	COD	1.51		-0.08^b	^{e}
6	H	H	COD		1.04^c	19.91^d	9, ^{e}
7	Me	Me	COD	0.92		20.15^b	^{e}
9	H	H	COD	0.74	1.34	29.00	^{e}, 8
11	Ph	Ph	COD	0.98		10.69^b	^{e}
12	H	H	$(CO)_2$	0.96	0.27	22.15	9, ^{e}
13	H	H	$(CO)_2$		0.43^c	26.48^d	9, ^{e}
14	H	H	$(CO)_2$	0.48	0.69	35.35	9, ^{e}
15	Indenyl potassium			1.52	0.63	24.24^e	^{e}
16	$[\eta^6$-$Cr(CO)_3$–indenyl$]^-K^+$			1.27	1.15	32.55^e	7
17	$[\eta^5$-$Cr(CO)_3$–indenyl$]^-K^+$			2.09	−0.09	17.51^e	7

[a] $\Delta^3J(H,H) = {}^3J_{H(4),H(5)} - {}^3J_{H(5),H(6)}$; $\Delta\delta(^1H) = \delta_{H(2)} - \delta_{H(1)}$; $\Delta\delta(^{13}C) = \delta_{C(2)} - \delta_{C(1)}$. For the complex identification, see Table 1. [b] The absolute value includes the effect of quaternization of C(1,3) nuclei. [c] Mean value between $\delta_{H(2)} - \delta_{H(1)}$ and $\delta_{H(2)} - \delta_{H(3)}$. [d] Mean value between $\delta_{C(2)} - \delta_{C(1)}$ and $\delta_{C(2)} - \delta_{C(3)}$. [e] This work.

$Cr(CO)_3$, in fact, on the paratropic [35] or diatropic [36] ring currents belonging to the whole molecule have been amply demonstrated.

Conclusions

The above considerations are in agreement with significant modifications of the electronic distribution in the indenyl moiety induced in the ground state by complexation with a 6π electron acceptor such as $Cr(CO)_3$. The indenyl–rhodium bond modifications induced by the presence of the second metal unit are responsible for the increased reactivity in the ligand exchange reactions (extra-indenyl effect) and of the catalytic and spectroscopic properties of the Rh center itself. This is confirmed by the increase of the free energy barrier measured [9] for the rotation of the Rh(COD) unit around the Rh–indenyl bond in the presence of Cr which correlates with the degree of distortion of the RhL_2 unit towards an η^3 bonding mode. Hence, the ground state energy of these bimetallic complexes is modified, e.g. by a weakening of the bond between Rh and the five-membered ring on going from an η^5 towards an η^3 coordination mode. Additionally, the reactivity of the Cr moiety towards strong $Cr(CO)_3$ acceptors is also increased in the presence of rhodium [9], which in turn indicates a reduced bond strength between the benzene ring and the Cr atom.

The modifications of both the coordinative bonds in the ground state of the bimetallic complexes can be represented by a fast equilibrium existing between the two isomers **I** and **II**, which differ in their hapticity.

$$\underset{\textbf{I}}{Cr(CO)_3(\eta^6{:}\eta^3\text{-indenyl})Rh\text{–}COD} \rightleftharpoons$$

$$\underset{\textbf{II}}{Cr(CO)_3(\eta^4{:}\eta^5\text{-indenyl})Rh\text{–}COD}$$

Therefore, the 'extra'-indenyl effect induced by $Cr(CO)_3$ should be accounted for (at least in part) by the increased allyl-ene character of the bonding of rhodium to the five-membered ring, which induces a decreased stability of the ground state of the bimetallic species.

Experimental

General

All reaction and complex manipulations were performed in an oxygen-free atmosphere. The solvents were carefully dried and deoxygenated before use. All complexes appear as microcrystalline air-stable powders, which gave satisfactory elemental analysis. Melting points are uncorrected. Microanalyses were performed by Mr L. Turiaco, Dipartimento di Chimica Inorganica, Metallorganica ed Analitica, Università di Padova. The IR spectra were recorded as CH_2Cl_2 solutions with a Perkin-Elmer 580B, and the 70 eV mass spectra were measured with a VG 16 Micromass spectrometer.

$Cr(CO)_3$–indenes

The parent [37] and the 3-Ph and 1,3-Ph_2 [38, 7] substituted indenes–$Cr(CO)_3$ have been previously described. The 3-Me– and 1,3-di-Me–indene–$Cr(CO)_3$ were obtained by reacting the ligand with

$(NH_3)_3Cr(CO)_3$ in refluxing dioxane for 4–6 h. Filtration and chromatography on silica of the reaction mixture gave the expected products.

(3-Methyl-indene)Cr(CO)$_3$

Yield 80%; m.p. 89–90 °C (from diethyl ether–pentane); ν_{max} (THF) (cm^{-1}): 1962, 1884 (C≡O); *m/z* 266 (M^+, 23.4%), 238 ($M^+ -$CO, 0.8), 210 ($M^+ -$2(CO), 13.3), 182($M^+ -$3(CO), 81.4), 130 ($M^+ -$(Cr, 3(CO)), 1.9), 115 ($M^+ -$(Cr, 3(CO), CH_3), 7.0) and 52 (Cr^+, 100). ^{1}H NMR ($CDCl_3$, ppm from internal Me_4Si): δ 6.15 (m, 1H, H-2), 5.80 and 5.66 (m, 1H each, H-4 and H-7, respectively), 5.25 (m, 2H, H-5 and H-6), 3.39 (m, 2H, H-1a and H-1b), 2.04 (m, 3H, 3-CH_3).

(1,3-Dimethyl-indene)Cr(CO)$_3$

Yield 42%; m.p. 78–80 °C (from diethyl ether–pentane); ν_{max} (THF) (cm^{-1}): 1959, 1880 (C≡O); *m/z* 280 (M^+, 19.3%), 252 ($M^+ -$CO, 0.6), 224 ($M^+ -$2(CO), 11.7), 196 ($M^+ -$3(CO), 80.0), 181 ($M^+ -$(3(CO), CH_3), 13.4), 144 ($M^+ -$(Cr, 3(CO)), 3.2), 129 ($M^+ -$(Cr, 3(CO), 2CH_3), 7.0) and 52 (Cr^+, 100). ^{1}H NMR ($CDCl_3$, ppm from internal Me_4Si): δ 6.08 (m, 1H, H-2), 5.75 and 5.58 (m, 1H each, H-4 and H-7, respectively), 5.26 (m, 2H, H-5 and H-6), 3.53 (m, 1H, H-1), 2.01 (m, 3H, 3-CH_3), 1.27 (d, ^3J 7.4 Hz, 1-CH_3).

Synthesis of the indenyl-Rh(COD) and Cr(CO)$_3$*–indenyl-Rh(COD) derivatives*

The indene derivatives were metallated at the appropriate temperature with excess KH as suspension in THF as previously reported [27, 39]. The ionization reaction was monitored by measuring the evolution of the hydrogen gas. The indenyl anion solution was then added to a THF solution of $[Rh(COD)Cl]_2$ maintained at the same temperature. The mixture was slowly warmed at r.t., the solvent removed at reduced pressure and the residue extracted several times with CH_2Cl_2. Crystallization of the bimetallic derivatives from CH_2Cl_2/pentane and of the monometallic ones from cyclohexane gave the desired products. The ^{1}H, ^{13}C and ^{103}Rh NMR chemical shift values are reported in Tables 1, 3 and 4, respectively.

Indenyl-Rh(COD). This compound has been previously reported [8].

1-Me–indenyl-Rh(COD). Yield 20%; m.p. 148–150 °C (decomp.); *m/z* 440 (M^+).

1,3-Me$_2$*–indenyl-Rh(COD).* Yield 73%; m.p. 150–153 °C (decomp.); *m/z* 454 (M^+).

1-C$_6$*H*$_5$*–indenyl-Rh(COD).* Yield 96%; m.p. 162–165 °C (decomp.); *m/z* 502 (M^+).

1,3-(C$_6$*H*$_5$*)*$_2$*–indenyl-Rh(COD).* Yield 72%; m.p. 169–173 °C (decomp.); *m/z* 578 (M^+).

5-NO$_2$*–indenyl-Rh(COD).* This compound has been previously described [9].

Cr(CO)$_3$*–indenyl-Rh(COD).* This compound has been previously described [8].

Cr(CO)$_3$*–(1-Me–indenyl)-Rh(COD).* Yield 40%; m.p. 169–172 °C (decomp.). ν_{max} (THF) (cm^{-1}): 1948vs, 1875vs, 1853vs (C≡O); λ_{max} (THF) (nm) (log ϵ): 253 (4.45), 349 (4.21) and 432 (3.86). *m/z* 476 (M^+, 30.6%), 420 ($M^+ -$2(CO), 38.3), 392 ($M^+ -$3(CO), 100), 340 ($M^+ -$(Cr, 3(CO)), 36.2), 325 ($M^+ -$(Cr, 3(CO), CH_3), 4.3), 232 ($M^+ -$(Cr, 3(CO), COD), 44.1), 217 ($M^+ -$(Cr, 3(CO), COD, CH_3), 1.9), 129 ($M^+ -$(Cr, 3(CO), Rh, COD), 4.8), 103 (Rh^+, 14.5), 52 (Cr^+, 45.2).

Cr(CO)$_3$*–(1,3-Me*$_2$*–indenyl)-Rh(COD).* Yield 90%; m.p. 173–176 °C (decomp.). ν_{max} (THF) (cm^{-1}): 1947vs, 1874vs, 1851vs (C≡O); λ_{max} (THF) (nm) (log ϵ) 257 (4.37), 348 (4.17), 435 (3.83). *m/z* 490 (M^+, 26.4%), 434 ($M^+ -$2(CO), 31.0), 406 ($M^+ -$3(CO), 100), 376 ($M^+ -$(3(CO), CH_3), 13.4), 354 ($M^+ -$(Cr, 3(CO)), 40.2), 339 ($M^+ -$(Cr, 3(CO), CH_3), 4.6), 324 ($M^+ -$(Cr, 3(CO), 2CH_3), 10.3), 246 ($M^+ -$(Cr, 3(CO), COD), 49.8), 216 ($M^+ -$(Cr, 3(CO), COD, 2CH_3), 5.7), 143 ($M^+ -$(Cr, 3(CO), Rh, COD), 4.1), 103 (Rh^+, 7.4), 52 (Cr^+, 41.7).

Cr(CO)$_3$*–(1-C*$_6$*H*$_5$*–indenyl)–Rh(COD).* Yield 76%; m.p. 178–181 °C (decomp.). ν_{max} (THF) (cm^{-1}): 1950vs, 1879vs, 1856vs (C≡O); λ_{max} (THF) (nm) (log ϵ): 257 (4.64), 323sh (4.32), 353 (4.36), 433 (4.01). *m/z* 538 (M^+, 12.6%), 454 ($M^+ -$3(CO), 44.1), 402 ($M^+ -$(Cr, 3(CO)), 100), 294 ($M^+ -$(Cr, 3(CO), COD), 84.8), 191 ($M^+ -$(Cr, 3(CO), Rh, COD), 23.4), 103 (Rh^+, 9.3), 52 (Cr^+, 62.4).

Cr(CO)$_3$*–(1,3-(C*$_6$*H*$_5$*)*$_2$*–indenyl)–Rh(COD).* Yield 79%. m.p. 186–190 °C (decomp.). ν_{max} (THF) (cm^{-1}): 1951vs, 1880vs, 1858vs (C≡O); λ_{max} (THF) (nm) (log ϵ): 270 (4.84), 292 (4.30), 325sh (4.19), 360 (4.12), 435 (3.78). *m/z* 614 (M^+, 6.1%), 530 ($M^+ -$3(CO), 24.1), 478 ($M^+ -$(Cr, (3CO)), 100), 370 ($M^+ -$(Cr, 3(CO), COD), 89.0), 267 ($M^+ -$(Cr, 3(CO), Rh, COD), 35.5), 103 (Rh^+, 3.4), 52 (Cr^+, 13.8).

Synthesis of the indenyl-Rh(CO)$_2$ *and Cr(CO)*$_3$*–indenyl-Rh(CO)*$_2$ *derivatives*

The appropriate Rh(COD) complexes were dissolved in CH_2Cl_2 and treated with CO. The reaction was monitored by TLC until the COD derivative had completely disappeared. The solvent was then removed by a stream of inert gas leaving a quantitative yield of orange–brown microcrystalline powder of high purity. The complexes indenyl-$Rh(CO)_2$ [11], 5-NO_2–indenyl-$Rh(CO)_2$ [9], and $Cr(CO)_3$–indenyl-$Rh(CO)_2$ [9] have already been described.

Collection of NMR data

Suitable 40–50 mmol dm^{-3} solutions for both ^{1}H and ^{13}C NMR measurements were obtained by using carefully dried, oxygen-free CD_2Cl_2. The proton spectra, recorded on a Bruker AM-400 spectrometer operating at 400.13 MHz, were analyzed using the Bruker PANIC program on a Bruker Aspect 2000 computer. For the NOE experiments, the samples were freed from oxygen by sonication under argon purging. The usual procedure for gated experiments was modified [27] and the selected multiplet was saturated by an 10 s cyclic perturbation of all lines with a 42 dB attenuation of a nominal 0.2 W decoupling power. The % enhancements were obtained from the multiplier of the reference spectrum which brings the multiplet to exact matching of the corresponding multiplet of the perturbed spectrum. Errors are *c.* 0.3%. The proton-decoupled 100.614 MHz ^{13}C NMR spectra were obtained on the same spectrometer by using a 6 s delayed Waltz-like CPD decoupling technique with full recovery of the Overhauser line enhancement to obtain satisfactory signal-to-noise ratios after 128–256 accumulations on a 64 K word size.

The ^{103}Rh NMR experiments (solvent, C_6D_6; T, 303 K) were performed on a Bruker AC-100 spectrometer equipped with a 10 mm ^{103}Rh, ^{31}P, ^{1}H probe, a second PTS 160 synthesizer provided with a 90° phase shifter, a BSV-3 heteronucleus decoupling unit with a selective amplifier for ^{103}Rh pulsing and a BVT 1000 temperature control (± 1 °C). Direct detection of ^{103}Rh is not possible at 2.35 Tesla, so all Rh NMR signals must be measured indirectly by using, for example, INEPT [40] or Inverse 2D experiments [12]. The ^{103}Rh frequencies were determined via Inverse 2D ^{1}H, ^{103}Rh using the pulse sequence [41]

$$90^\circ_{(^1\mathrm{H})} - [2J_{(^{103}\mathrm{Rh},\,^1\mathrm{H})}]^{-1} - 90^\circ_{(^{103}\mathrm{Rh})} - t_1/2$$
$$- 180^\circ_{(^1\mathrm{H})} - t_1/2 - 90^\circ_{(^{103}\mathrm{Rh})} - \mathrm{AQT}_{(^1\mathrm{H})}$$

The 90° ^{103}Rh pulse was 30 μs and the 90° ^{1}H pulse was 26 μs. A 16-step phase cycling was employed, giving quadrature detection in the F1 dimension and eliminating the proton signals in F2 which are not coupled to Rh by approximately the J(input), i.e. $J(\mathrm{Rh, H(2)}) \approx 2\mathrm{Hz}$. In the first experiment for every compound the ^{103}Rh carrier frequency was set approximately in the centre of the Rh(I) frequency range (3.136 MHz), the spectral range in F1 was set at 10 000 Hz and 128 t_1 increments were recorded. The experiment was then repeated with the ^{103}Rh frequency set nearly on resonance, the spectral range of the F1 dimension was set at 1000 Hz and 256 t_1 increments were taken, giving a spectral resolution better than ± 2 Hz per point for ^{103}Rh. The spectral width of the ^{1}H dimension was set as narrow as possible for 512 word memory, the relaxation delay was 6 s and two dummy scans were taken. This led to an experimental time of 10 h, but good spectra can also be obtained within 2 h (resolution ± 6 Hz per point). After zero-filling once in both dimensions, the 512×1024 w matrix was processed in the usual manner. The $\delta(^{103}\mathrm{Rh})$ values were calculated by determining the absolute ^{103}Rh frequency of the cross peaks and relating it to the arbitrary reference frequency of 3.16 MHz (Ξ value at 100.00 MHz) which is 3.16415 MHz for operation at 100.13 MHz ^{1}H frequency.

Acknowledgements

This work was supported in part by the Consiglio Nazionale delle Ricerche (Roma) through its 'Centro di Studio sugli Stati Molecolari, Radicalici ed Eccitati', and by the Netherlands Foundation for Chemical Research (SON).

References

1 J. M. Connor and C. P. Casey, *Chem. Rev.*, *87* (1987) 307; J. W. Faller, R. H. Crabtree and A. Habib, *Organometallics*, *4* (1985) 929.
2 A. Borrini, P. Diversi, G. Ingrosso, A. Lucherini and G. Serra, *J. Mol. Catal.*, *30* (1985) 181, and refs. therein.
3 M. E. Rerek, L. N. Ji and F. Basolo, *J. Chem. Soc., Chem. Commun.*, (1983) 1208; L. N. Ji, M. E. Rerek and F. Basolo, *Organometallics*, *3* (1984) 740.
4 A. J. Hart-Davis and R. J. Mawby, *J. Chem. Soc. A*, (1969) 2403; A. J. Hart-Davis, C. White and R. J. Mawby, *Inorg. Chim. Acta*, *4* (1970) 441; D. J. Jones and R. J. Mawby, *Inorg. Chim. Acta*, *6* (1972) 157.
5 (a) S. A. Wescott, A. K. Kakkar, G. Stringer, N. J. Taylor and T. B. Marder, *J. Organomet. Chem.*, *394* (1990) 777, and refs. therein; (b) F. H. Köhler, *Chem. Ber.*, *107* (1974) 570.
6 G. J. Kubas, G. Kiss and C. D. Hoff, *Organometallics*, *10* (1991) 2870.
7 A. Ceccon, A. Gambaro, F. Gottardi, S. Santi and A. Venzo, *J. Organomet. Chem.*, *412* (1991) 85.
8 A. Ceccon, A. Gambaro, S. Santi, G. Valle and A. Venzo, *J. Chem. Soc., Chem. Commun.*, (1989) 51.
9 A. Ceccon, A. Gambaro, S. Santi and A. Venzo, *J. Mol. Catal.*, *69* (1991) L1.
10 S. Bellomo, C. Bonifaci, A. Ceccon, A. Gambaro, S. Santi and A. Venzo, *Abstr., XVth Int. Conf. Organometallic Chemistry, Warsaw, Poland, Aug. 9–14, 1992*, pp. 0–51.
11 A. K. Kakkar, N. J. Taylor, J. C. Calabrese, W. A. Nugent, D. C. Roe, E. A. Connaway and T. B. Marder, *J. Chem. Soc., Chem. Commun.*, (1989) 990.
12 (a) R. Benn, H. Brenneke and A. Rufinska, *J. Organomet. Chem.*, *320* (1987) 115; (b) A. A. H. van der Zeÿden, G. van Koten, C. J. Elsevier, J. M. Ernsting, B. Krÿnen and C. H. Stam, *J. Chem. Soc., Dalton Trans.*, (1989) 317; (c) C. J. Elsevier, J. M. Ernsting and W. J. de Lange, *J. Chem. Soc., Chem. Commun.*, (1989) 585.
13 B. E. Mann, in *NMR of Newly Accesible Nuclei*, Academic Press, New York, 1983, Ch. 11.
14 W. von Philipsborn, *Pure Appl. Chem.*, *58* (1986) 513.
15 R. D. Reinhardt, *Thesis*, Ruhr Universität, Bochum, 1985.

16 H. Adams, N. A. Bayley, B. E. Mann, B. F. Taylor, C. White and P. Yavari, *J. Chem. Soc., Dalton Trans.*, (1987) 1947.

17 H. Bönneman and W. Brijoux, *Aspects Homog. Catal.*, *5* (1984) 94.

18 P. B. Graham, M. D. Rausch, K. Täschler and W. von Philipsborn, *Organometallics, 10* (1991) 3049.

19 J. D. Holmes, D. A. K. Jones and R. Pettit, *J. Organomet. Chem.*, *4* (1965) 324; G. Klopman and F. Calderazzo, *Inorg. Chem.*, *6* (1967) 977; R. S. Bly and R. L. Veazey, *J. Am. Chem. Soc.*, *91* (1969) 4221; R. S. Bly, R. C. Strickland, R. T. Swindell and R. L. Veazey, *J. Am. Chem. Soc.*, *92* (1970) 3722; P. J. Dossor, C. Eaborn and D. R. M. Walton, *J. Organomet. Chem.*, *71* (1974) 207; A. Ceccon and G. Catelani, *72* (1974) 79, and preceeding papers of the series.

20 B. Nicholls and M. C. Whiting, *J. Chem. Soc.*, (1959) 551; W. S. Trahanovsky and D. K. Wells, *J. Am. Chem. Soc.*, *91* (1969) 5870, 5871; A. Wu, E. R. Biehl and P. C. Reeves, *J. Organomet. Chem.*, *33* (1972) 53; *J. Chem. Soc., Perkin Trans. II*, (1972) 449.

21 A. K. Kakkar, S. F. Jones, N. J. Taylor, S. Collins and T. B. Marder, *J. Chem. Soc. Chem. Commun.*, (1989) 1454.

22 F. H. Köhler, *Chem. Ber.*, *107* (1976) 273.

23 R. T. Baker and T. H. Tulip, *Organometallics, 5* (1986) 839.

24 T. B. Marder, J. C. Calabrese, D. C. Roe and T. H. Tulip, *Organometallics, 6* (1987) 2012; R. T. Carl, R. P. Hughes, A. L. Rheingold, T. B. Marder and N. J. Taylor, *Organometallics, 7* (1988) 1613.

25 J. S. Merola, R.-T. Kacmarcik and D. Van Engen, *J. Am. Chem. Soc.*, *108* (1986) 329.

26 T. C. Forschner, A. R. Cutler and R. K. Kullnig, *Organometallics, 6* (1987) 889.

27 A. Ceccon, A. Gambaro, A. Venzo, V. Lucchini, T. E. Bitterwolf and J. Shade, *J. Organomet. Chem.*, *349* (1988) 315, and refs. therein.

28 A. Ceccon, A. Gambaro, A. M. Romanin and A. Venzo, *J. Organomet. Chem.*, *239* (1982) 345.

29 R. D. Rogers, J. L. Atwood, T. A. Albright, W. A. Lee and M. D. Rausch, *Organometallics, 3* (1984) 263.

30 A. Ceccon, A. Gambaro, A. M. Romain and A. Venzo, *J. Organomet. Chem.*, *254* (1983) 199.

31 A. Ceccon, A. Gambaro and A. Venzo, *J. Chem. Soc., Chem. Commun.*, (1985) 540.

32 A. Ceccon, A. Gambaro, F. Gottardi, S. Santi, A. Venzo and V. Lucchini, *J. Organomet. Chem.*, *379* (1989) 67.

33 S. A. King, D. Van Engen, H. E. Fischer and J. Schwartz, *Organometallics, 10* (1991) 1195.

34 F. Coletta, A. Gambaro, G. Rigatti and A. Venzo, *Spectroscop. Lett.*, *10* (1977) 971.

35 A. Ceccon, A. Gambaro, L. Pizzato, A. M. Romanin and A. Venzo, *J. Chem. Soc., Chem. Commun.*, (1982) 907; A. Ceccon, A. Gambaro and A. Venzo, *J. Organomet. Chem.*, *281* (1985) 221.

36 A. Ceccon, A. Gambaro, A. M. Romanin and A. Venzo, *Angew. Chem., Int. Ed. Engl.*, *22* (1983) 559; *Angew. Chem. Suppl.*, (1983) 734.

37 A. N. Nesmeyanov, N. A. Ustynyuk, L. G. Makarova, S. Andre, Yu. A. Ustynyuk, L. N. Novikova and Yu. N. Luzikov, *J. Organomet. Chem.*, *154* (1978) 45.

38 P. Berno, A. Ceccon, A. Gambaro and A. Venzo, *Tetrahedron Lett.*, *29* (1988) 3849.

39 A. Ceccon, A. Gambaro, A. Venzo, V. Lucchini, T. E. Bitterwolf and J. Shade, *J. Organomet. Chem.*, *327* (1987) 55.

40 (a) C. Brevard and R. Schimpf, *J. Magn. Reson.*, *47* (1982) 47, 528; (b) M. Kinns and J. K. M. Sanders, *J. Magn. Reson.*, *56* (1984) 518.

41 A. Bax, R. H. Griffey and B. L. Hawkins, *J. Magn. Reson.*, *55* (1983) 301.